Peter VIRTIČ[1]

University of Maribor, Faculty of Energy Technology (1)

Variations of Permanent Magnets Dimensions in Axial Flux Permanent Magnet Synchronous Machine

Abstract. *This paper presents the variations of permanent magnets (PMs) dimensions in axial flux permanent magnet synchronous machine (AFPMSM). By the variation of PMs dimensions the influences on the machine characteristics are researched by using analytical method via magnetic vector potential. The results obtained by analytical method are confirmed by using finite element method (FEM) and measurements.*

Streszczenie. *W artykule zaprezentowano zmiany wymiarów magnesu stałego w osiowym silniku synchronicznym. Wpływ tych zmian oceniono analitycznie metoda potencjału wektorowego. Wyniki są zgodne z obliczeniami metodą elementu skończonego oraz z eksperymentem. (**Zmiany wymiarów magnesu stałego w osiowym silniku synchronicznym**)*

Keywords: synchronous machine, permanent magnet, axial flux, magnetic field.
Słowa kluczowe: silnik synchroniczny, strumień magnetyczny.

Introduction

Since the permanent magnets (PMs) material price reduced significantly the research activities in the field of axial flux permanent magnet machines greatly increased. Axial flux permanent magnet synchronous machines (AFPMSMs) became an attractive solution to increase power densities of electrical machines. The electrical machines industry showed a great interest for such improvement in order to achieve smaller machine weight and size or higher power at the same machine size. Moreover, AFPMSMs can be built into the applications where conventional machines cannot be built in due to the constraints in the axial direction. By increasing the machine radius the advantage of AFPMSMs, compared with radial flux counterparts, becomes more expressive, especially when using NdFeB PMs. On the other hand, the PMs are the most expensive parts of electrical machines. Therefore, it is convenient to study the influence of the amount of PMs on AFPMSM characteristics. In this paper the impact of PMs dimensions on static characteristics of AFPMSM with double external rotor and coreless stator is presented (Fig. 1). These characteristics are calculated by using analytical method via magnetic vector potential.

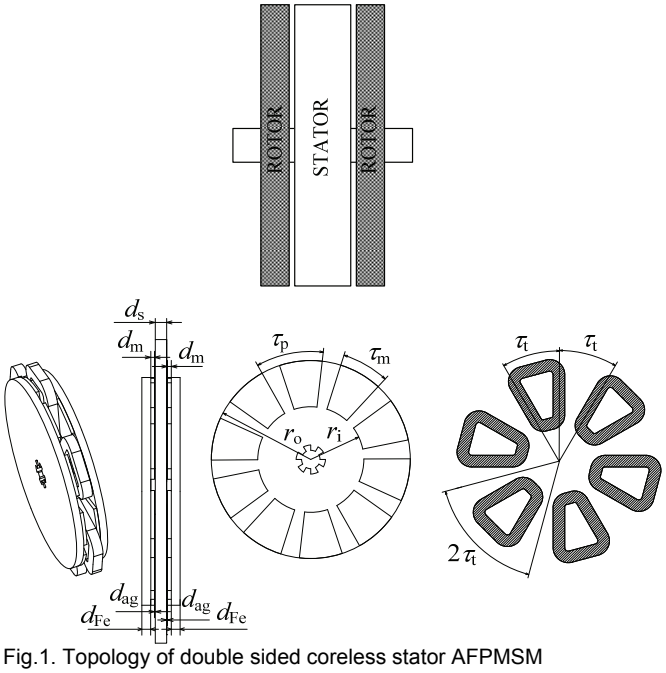

Fig.1. Topology of double sided coreless stator AFPMSM

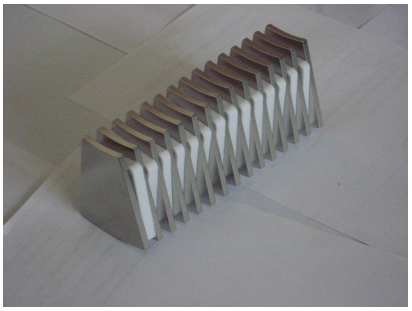

Fig.2. Permanent magnets

Calculation of the dynamic characteristics requires the employment of a dynamic model. The model may be either magnetically non-linear with defined parameters in a non-linear manner [1], or it may be linear with either variable or constant parameters, depending on the required drive performance and accuracy [2,3].

Method of analysis

Method of analysis is based on the derived equations in explicit forms for the magnetic field calculation by using analytical method via magnetic vector potential [4]. AFPMSM characteristics can therefore be calculated by using method based on the Maxwell's equations (1), (2) and constitutive equation (3) considering (4).

$$\nabla \times \boldsymbol{H} = \boldsymbol{J}_{\mathrm{f}} \tag{1}$$

$$\nabla \cdot \boldsymbol{B} = 0 \tag{2}$$

$$\boldsymbol{B} = \mu_{\mathrm{r}} \mu_0 \boldsymbol{H} + \mu_0 \boldsymbol{M} \tag{3}$$

where: $\boldsymbol{J}_{\mathrm{f}}$ – free volume current density due to the movement of free charges, μ_0 – permeability of free space, μ_{r} – relative permeability of the associated region, $\boldsymbol{B}$ – magnetic flux density, $\boldsymbol{H}$ – magnetic field intensity, $\boldsymbol{M}$ – residual magnetization vector.

$$\boldsymbol{B} = \nabla \times \boldsymbol{A} \tag{4}$$

Solving the system of equations (1-4) yields the vector Poisson equation:

$$\nabla^2 \boldsymbol{A} = -\mu_0 \left(\mu_{\mathrm{r}} \boldsymbol{J}_{\mathrm{f}} + \nabla \times \boldsymbol{M} \right) \tag{5}$$

Due to the ironless stator and therefore magnetically linear materials, the final whole magnetic flux density can be obtained by the superposition of magnetic flux densities

produced by PMs and armature current. During the derivation procedure, the infinite permeability of back iron in rotor discs is assumed. In the equation (5) the first term on the right-hand side represents the excitation produced by armature current while the second term represents the excitation produced by PMs.

For static torque (T) and attractive force (F_z) calculations the Maxwell's stress tensor method is used as follows in (6) and (7), respectively.

$$T = \frac{1}{\mu_0}\int_S B_\varphi B_z \mathrm{d}S \tag{6}$$

$$F_z = \frac{1}{2\mu_0}\int_S \left(B_z^2 - B_\varphi^2\right)\mathrm{d}S \tag{7}$$

where: B_z – axial component of magnetic flux density, B_φ – circumferential component of magnetic flux density, S – integration surface, which is chosen at the centre of air-gap.

The back electromotive force (EMF) of the AFPMSM has been calculated using Faraday's law of electromagnetic induction based on the time variation of magnetic flux as:

$$e = -N\frac{\mathrm{d}\phi}{\mathrm{d}t} \tag{8}$$

where: N – number of turns, e – back EMF, $\mathrm{d}\phi/\mathrm{d}t$ – time variation of magnetic flux within the coil.

Results and discussion

The amount of PMs is determined by their dimensions such as thickness (d_m), length (r_o-r_i) and width (τ_m). The comparisons between back EMF waveforms in Fig. 2 show the maximum magnitude at inner radius of 40 mm. Fig. 3. shows the maximum torque at inner radius of 10 mm, but it is also clearly shown that static torque amplitude at inner radius of 40 mm is slightly lower than at 10 mm. Maximum static torque according to displacement and PM angle increases asymptotically by increasing τ_m. For this reason, it is more convenient and cost effective to limit amount of PMs with dimensions which considerably contribute to higher amplitude of static torque and back EMF characteristics.

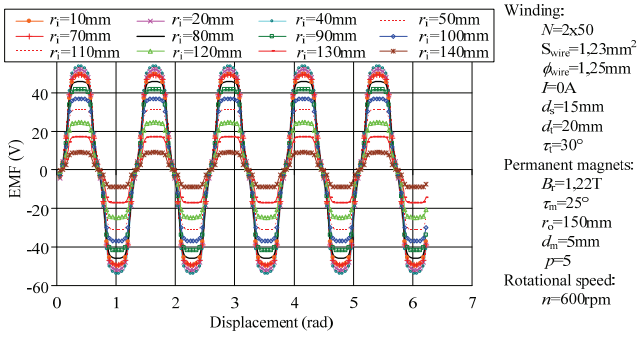

Fig.3. Electromotive force according to displacement and inner radius of PMs

Fig. 2 presents back EMF according to displacement at different inner radius (r_i), while all other dimensions and parameters of the machine parts remain constant. In addition, the PM length is changing but the outer radius of PM remains constant as well as the outer machine radius. The shortest length of PMs is 10 mm, which cover only 10 mm length of coils sides. Due to the shortest length of coil sides the lowest amplitude of back EMF waveform is induced. When observing figures presenting back EMF it has to be considered that coils sides length coincides with the PMs length.

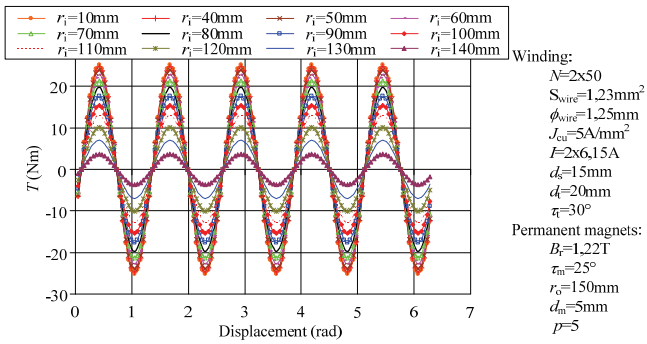

Fig.4. Static torque according to displacement and inner radius of PMs

Static torque according to displacement and different inner radius of PMs is presented in Fig. 4. It can be actually seen that increasing the length of the PMs does not proportionally contribute to the static torque (T) neither to the back EMF amplitude.

Fig. 5 presents the dependency of static torque according to rotational angle and PMs angle (τ_m). By increasing the angle of PMs the amount of PMs is increasing but on the other hand the distance between adjacent PM is smaller. For this reason more magnetic flux flows directly to the adjacent PMs instead of flowing through the stator to the other iron disc of double external rotor.

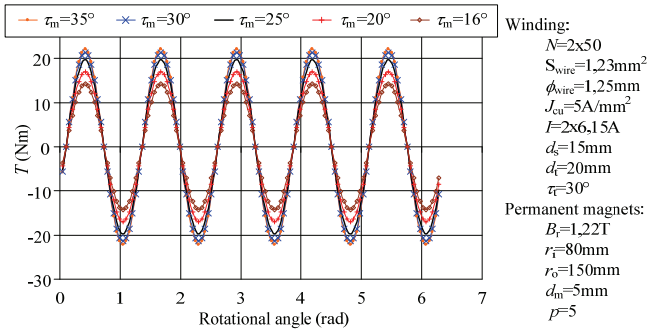

Fig.5. Static torque according to displacement and PM angle

Fig. 6 presents electromotive force according to displacement and PMs angle. Unlike the amplitude of static torque (Fig. 5) the amplitude of back EMF remains the same by increasing the PMs angle but the width of EMF wave is increasing.

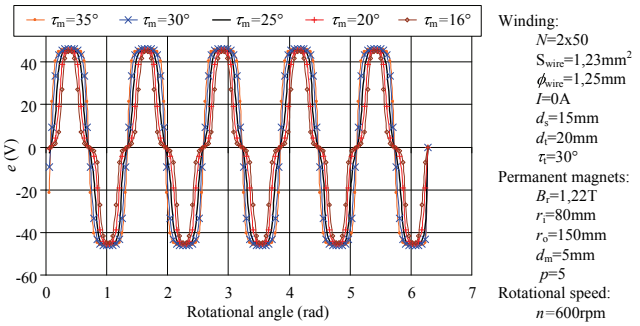

Fig.6. Electromotive force according to displacement and PM angle

In order to maximize the output power for specific loadings, the ratio of r_o to r_i should be chosen to be $\sqrt{3}$. This

ratio fits the most to the inner radius of 80 or 90 mm at outer radius 150 mm. For this reason and the reason of lower costs the PMs with 80 mm of inner radius were chosen for prototype AFPMSM.

Although the size of AFPMSM is constrained and therefore diameter of external rotor, which has to be 300 mm, the dependency of back EMF and static torque according to the rotational angle and outer radius is presented as well, while the inner radius of PMs remains constant at 80 mm.

Fig. 7 presents the rise of back EMF waveform amplitude by increasing the outer radius according to rotational angle.

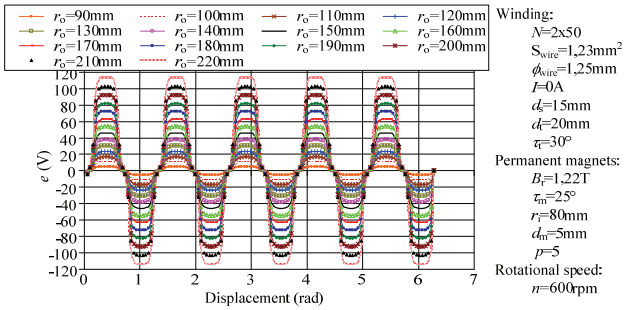

Fig.7. Back EMF according to displacement

Fig. 8 presents static torque in dependency on displacement and outer rotor radius. By increasing the rotor radius the considerable contribution of static torque amplitude is achieved.

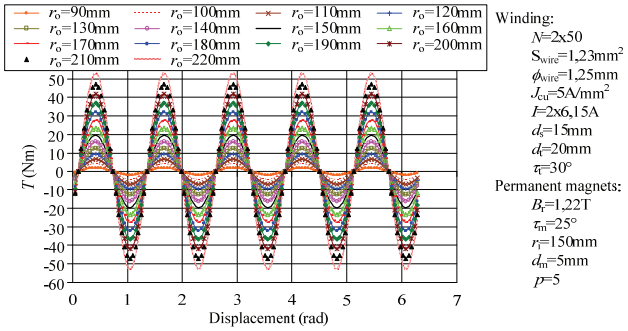

Fig.8. Static torque according to displacement

Two important advantages of AFPMSM with longer diameter can be figured out. The first one is more space for PMs and stator coils and the second is higher torque due to the longer machine radius.

The last dimension of PMs to vary, in order to observe the influence on the AFPMSM characteristics, is PMs thickness (d_m).

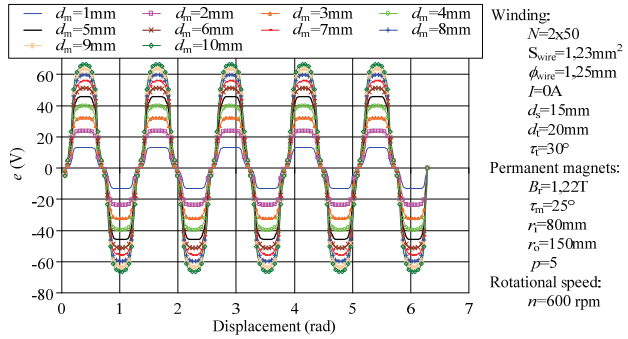

Fig.9. Back EMF according to displacement

Back EMF and static torque in dependency on displacement are presented in Fig. 9 and Fig. 10, respectively. Furthermore, normal and tangential component of magnetic flux density in dependency on circumferential coordinate and PMs thickness are presented below.

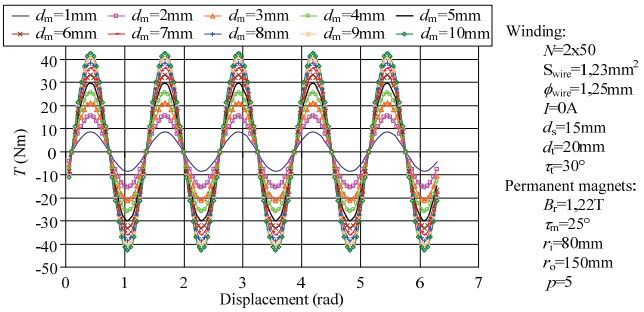

Fig.10. Static torque according to displacement

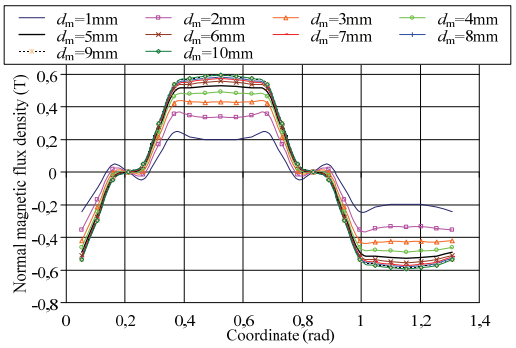

Fig.11. Normal component of magnetic flux density by PMs in dependency on circumferential coordinate (analytical method)

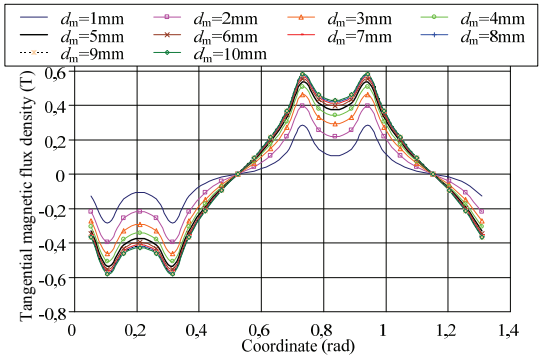

Fig.12. Tangential component of magnetic flux density by PMs according to circumferential coordinate (analytical method)

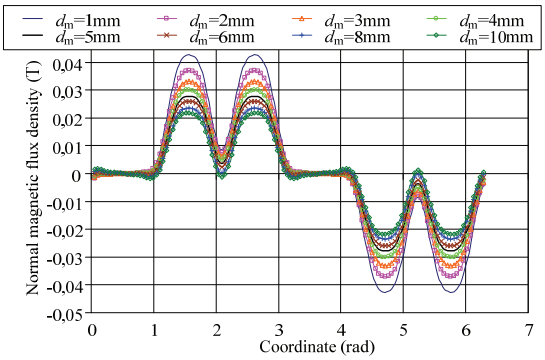

Fig.13. Normal component of magnetic flux density by armature current according to circumferential coordinate (analytical method)

By increasing the PMs thickness the back EMF amplitude is increased, but the dependency is not proportional due to the rise of equivalent air-gap between

both rotor iron discs as well. For this reason the amplitude of normal (Fig. 11) and tangential component of magnetic flux density (Fig. 12) produced by PMs asymptotically decreases by increasing the PMs thickness. According to these characteristics and lower price of PMs produced in bigger series 5 mm of PMs thickness is chosen for the AFPMSM of 300 mm rotor diameter.

PMs thickness influences also on the normal (Fig. 13) and tangential (Fig. 14) magnetic flux density distribution due to the armature current. Due to the relative permeability of PMs, which is slightly higher than one, the rise of equivalent air-gap length appears by increasing the PMs thickness.

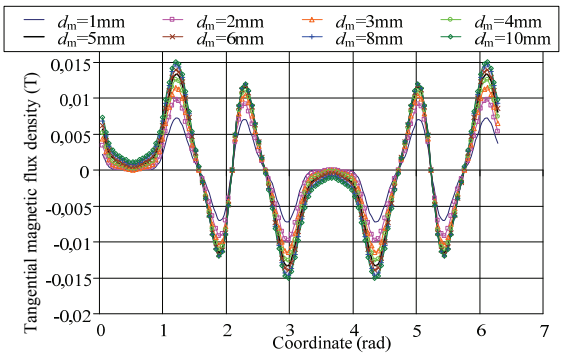

Fig.14. Tangential component of magnetic flux density by armature current according to circumferential coordinate (analytical method)

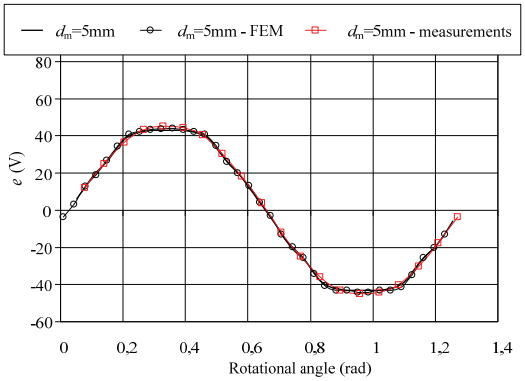

Fig.15. Verification of the analytical method with FEM and measurements on prototype AFPMSM

In order to obtain reliable results the verification of analytical method via magnetic vector potential was accomplished. In Fig. 15 the analytically calculated back EMF is validated with measurements on prototype AFPMSM and FEM by using Ansys programme package.

Conclusion

The results obtained by analytical method are in good agreement with the results obtained by FEM and measurements.

The main advantage of the analytical method is a shorter computational time and flexible computation for the back EMF and torque calculation in comparison to FEM. It also enables direct insight in the machine design. Due to the short computational time the analytical method is the most convenient, especially for early design stages.

REFERENCES

[1] Hadžiselimović M., Štumberger G., Štumberger B., Zagradišnik I.,"Magnetically nonlinear dynamic model of synchronous motor with permanent magnets," *J. Magn. Magn. Mater.*, 316 (2007), e257-e260.

[2] Štumberger B., Štumberger G., Hadžiselimović M., Trlep M., Hamler A., "Permanent magnet brushless DC motor - integrated motor drive electrical subsystem simulation", *Prz. Elektrotech*., 83 (2007), No. 7-8, 135-138.

[3] Štumberger B., Goričan V., Štumberger G., Hadžiselimović M., Marčič T., Trlep M., "Performance evaluation of synchronous reluctance motor in BLDC drive", *Prz. Elektrotech.,* 85 (2009), No. 12, 147-149.

[4] Virtič P., Pišek P., Štumberger B., Bojan, Hadžiselimović M., Marčič T., Praunseis Z., "Winding design of coreless stator axial flux permanent magnet synchronous machines", *Prz. Elektrotech.,* 85 (2009), No. 12, 162-165.

[5] T.F. Chan, L. L. Lai, An Axial-Flux Permanent-Magnet Synchronous Generator for a Direct-Coupled Wind-Turbine System, *Transactions on Energy Conversion*, 22 (2007), No. 1, 86-94.

[6] Gieras J.F., Kamper M.J., Wang R.-J., Axial Flux Permanent Magnet Brushless Machines, Springer, 2008.

***Author**: asst. prof. Peter Virtič, Ph.D., University of Maribor, Faculty of Energy Technology, Hočevarjev trg 1, 8270 Krško, E-mail: peter.virtic@uni-mb.si.*